Development of a Microchannel Plate Based Beam Profile Monitor for Re-accelerated Muon Beam

Bongho Kim[a,b], Sunghan Bae[a,b], Hyunsuk Choi[a,b], Seonho Choi[a,b], Naritoshi Kawamura[g,h], Ryo Kitamura[c], Ho San Ko[a,b], Yasuhiro Kondo[j], Tsutomu Mibe[d], Masashi Otani[d], Georgiy P. Razuvaev[e,f], Eunil Won[i]

[a]*Department of Physics and Astronomy, Seoul National University, Seoul, 08826, Korea*
[b]*Institute for Nuclear and Particle Astrophysics, Seoul National University, Seoul, 08826, Korea*
[c]*Department of Physics, University of Tokyo, Tokyo 113-0033, Japan*
[d]*High Energy Accelerator Research Organization (KEK), Tsukuba 305-0801, Japan*
[e]*Budker Institute of Nuclear Physics SB RAS, Novosibirsk 630090, Russia*
[f]*Novosibirsk State University, Novosibirsk 630090, Russia*
[g]*Muon Sci. Lab., Institute of Materials Structure Science, High Accelerator Research Organization, Tsukuba, 305-0801, Japan*
[h]*Muon Sci. Sec., Materials and Life Science Facility, J-PARC, Tokai, 319-1195, Japan*
[i]*Department of Physics, Korea University, Seoul, 02841, Korea*
[j]*Japan Atomic Energy Agency (JAEA), Tokai, 319-1195, Japan*

Abstract

A beam profile monitor (BPM) based on a microchannel plate has been developed for ultracold muon beams for the measurement of the muon anomalous magnetic moment and electric dipole moment at high precision, with capability of diagnosing muon beams of energy range from a few keV to 4 MeV. The performance of the BPM has been evaluated using a surface muon beam at J-PARC and additionally with a UV light source. It has been confirmed that the BPM has a dynamic range from a few to 10^4 muons per bunch without saturation. The resolution of the BPM has been estimated to be less than 0.30 mm. A partial discrimination of positrons from muons has been achieved under discrete particle conditions.

Keywords: Ultracold muon, Beam diagnostics, Microchannel Plate, Beam profile

1. Introduction

The J-PARC muon $g - 2$/EDM experiment [?] aims to measure the muon anomalous magnetic moment ($a_\mu = (g - 2)_\mu/2$) and the muon electric dipole moment (EDM) with high precision. A new beam line for muons (H-line) [?] is under development. The experiment requires a muon beam with small transverse emittance that is obtained by re-accelerating ultraslow muons. The ultraslow muons are produced from ionization of muonium ($\mu^+ e^-$) at thermal energy with lasers. Muonium is produced by stopping a surface muon beam in a muonium production target [?]. This muon beam with low transverse momentum will be re-accelerated to 300 MeV/c [?] while minimizing the increase of the transverse momentum ($\sigma_{pT}/p = 10^{-5}$). The accelerated muon beam is injected to the storage area under 3 T magnetic field without electric focusing [?]. The experiment measures $g - 2$ with a precision of 0.1 ppm and the EDM with a sensitivity to $10^{-21}\, e \cdot$ cm. Proper beam diagnostics are required for the development of this new muon beam.

In contrast to other surface muon monitors [? ?], the BPM is designed to measure a beam profile and relative intensity for each bunch simultaneously from low intensity (a few muons per bunch) to high intensity in the energy range from a few keV to 4 MeV. A BPM based on a Micro-Channel Plate (MCP) has been developed to obtain necessary gain and efficiency to measure a low intensity beam. There have been several experiments that have used detectors based on an MCP assembly to
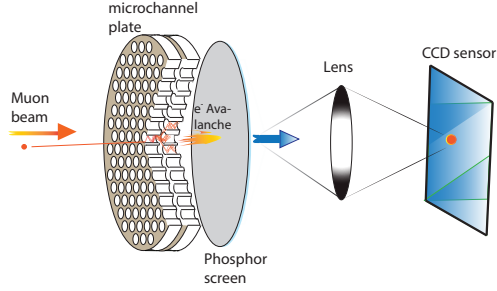
Figure 1: A schematic view of the BPM.

work with beams of muons, neutrons, ions, atoms and positronium [? ? ?]. Unlike other beams, muons are stopped in the MCP due to a short penetration depth and decay to positrons plus muon antineutrinos and electron neutrinos by the weak interaction. These positrons give signals in the BPM via penetration of the MCP channels. Understanding and subtracting this positron background from the muon signal is one of the challenges in measuring a precise beam profile.

In this paper, we present the design and results of tests using the surface muon beam and the UV light source. The responses of muon and positron signals and the signal linearity were measured by the surface muon beam. The spatial resolution was measured by a UV light with a semicircular hole collimator.

2. BPM design and specification

The BPM is designed to characterize a muon beam with sub-millimeter resolution for a $\sim$10 mm beam spot size for the energy range from a few keV to 4 MeV corresponding to the low β section of the muon LINAC [?]. The BPM aims to measure a muon intensity from a few muons to 10^5 muons per bunch at a repetition rate of 25 Hz.

As shown in Fig. 1, the BPM consists of two stages of MCP, one stage of a phosphor screen and a CCD camera. High efficiency for keV order atomic and ion beams has been observed in several experiments [? ?]. Similar high efficiency for a low energy muon beam is expected.

The MCP assembly (Hamamatsu F2225-21P) has two stages of chevron type MCPs with an effective area corresponding to a diameter of $\varnothing = 40$ mm and gain of 10^6–10^7 plus a phosphor screen (P47).

The light output from the phosphor screen is transmitted through a glass viewport (7056 borosilicate) and then captured by the cooled CCD camera (PCO PCO1600: 800×600 pixels with combined 2×2 binning mode) with lens (Zeiss Distagon 2/28 ZF.2). In order to block the electron background, negative potential (-1.9 kV) is applied in the MCP front surface. The MCP back surface is connected to a ground after an electric circuit to read out the electric signal of the MCP. Positive potential (3.9 kV) is applied to the phosphor screen.

The exposure time of the CCD camera is set to $0.5\,\mu$s to reject positrons from the muon decay ($\tau = 2.2\,\mu$s [?]). The P47 phosphor material is chosen to have a short decay time ($\tau_{10\,\%} = 0.11\,\mu$s) compared to the exposure time to enable this discrimination method.

The MCP assembly is installed in the middle of a cylindrical vacuum chamber constructed from stainless steel. The MCP assembly and the CCD camera are aligned in the cylindrical axis. The vacuum chamber has a thin mylar film (0.1 mm) window with $\varnothing = 100$ mm in a flange in front of the MCP assembly for beam transmission. Another mylar film window is installed in a side port for positron transmission. There is a viewport in a flange behind the MCP assembly.

3. Experiment with muon beam

3.1. Experimental setup

A schematic view of the experimental setup for the surface muon beam test is shown in Fig.2. The J-PARC muon facility provides surface muons (μ^+) as a pulsed beam to the Material and Life Science Experimental Facility (MLF) D-line D2 area with 100 ns beam width, 4 MeV kinetic energy, and 25 Hz repetition rate [? ?]. The beam intensity was adjusted by slits in the beamline. The beam size and intensity was further adjusted by installing one of a set of lead collimators with $\varnothing = 10$ mm, 20 mm or 40 mm hole between the exit window of the beam line and the BPM vacuum chamber. The MCP assembly was installed inside the BPM vacuum chamber which was separated from the beam line as an independent vacuum system.

The number of muons on the BPM was measured from decay positrons. Some of the decay positrons from muons stopped in the MCP volume go through the mylar film in the side port of the BPM chamber and give signals to the positron counter. The
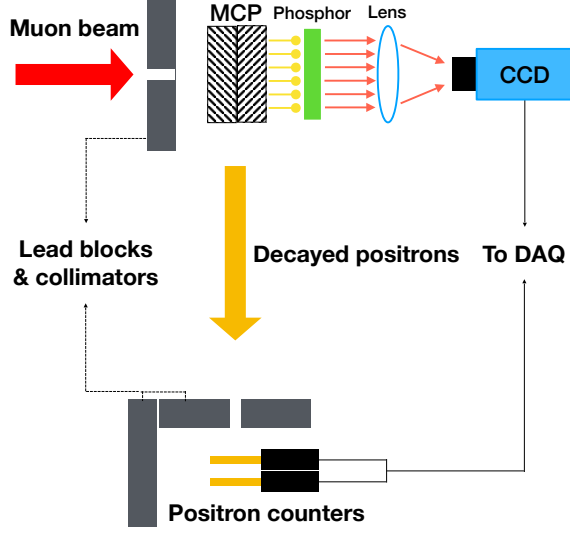
2

Figure 2: Setup for the test with muon beam at the J-PARC MLF D-line D2 area.

Figure 3: Typical CCD images taken with muon beam. (a) single picture at high intensity. (b) accumulation of 1,000 pictures. (c) single picture with low intensity. (d) single picture of $2\,\mu$s delayed trigger timing. The pixels with higher ADC counts are in white. Dashed lines are artificial drawing of MCP boundary.

number ratio of such positrons and muons on the BPM is determined by the simulation as described in data analysis part. The positron counter consists of two plastic scintillators with corresponding light guides and PMTs. The positron counter was shielded by lead blocks to suppress decay positrons from directions other than from the MCP. A lead collimator with a $\varnothing = 30\,$mm hole was used to provide a direct view of the MCP from the positron counter.

3.2. Data taking

Two dimensional pictures were taken by the CCD camera with $500\,$ns exposure time. The arrival time of the muon beam was measured by the electronic signal of the MCP. This timing information was used to set the proper timing for triggering the CCD exposure. The waveform data for the positron counter was taken for a $10\,\mu$s period in coincidence with the muon beam pulse.

Data with a few muons per pulse were taken to understand the properties of a single muon signal. Data with higher intensities were then taken by changing the sizes of the slit in the beam line and the collimator. Another set of data was taken with different trigger timing for the CCD camera to understand positron signals in the BPM. Typical CCD images taken at different intensities are displayed in Fig. 3. A raw picture (Fig. 3a) and the accumulation of 1000 pictures in a two dimensional histogram (Fig. 3b) were taken with the high intensity muon beam. Low intensity pictures are shown for muon arrival time (Fig. 3c) and delayed trigger timing by $2\,\mu$s (Fig. 3d).

3.3. Data analysis

As shown in Fig. 3, the signals are distinguishable from the CCD noise. To analyze the signals from CCD noise, a cluster is defined for single signal selection. A single cluster region for each signal is defined as 9×9 pixels from the pixel with maximum ADC count in each signal. This region is about 5 times of root mean square (RMS) width (1.6 pixel) of a single muon signal. In the data, the 40 mm MCP diameter corresponds to 500 pixels, resulting in a scale of 0.08 mm/pixel.

Each cluster is identified by detecting 3×3 pixels which satisfy that ADC value in each pixel is larger than mean CCD noise of corresponding pixel by thresholds determined from the noise fluctuation ($\sigma =8.7\,$ADC) which is averaged over all pixels. The properties of single clusters are studied with this selection criterion.

The distribution of the cluster ADC sum is displayed in Fig. 4. The ADC sum distribution shows an isolated peak for exposure to muons, with no corresponding peak for delayed exposure ($t_{delay} = 2, 3\,\mu$s).

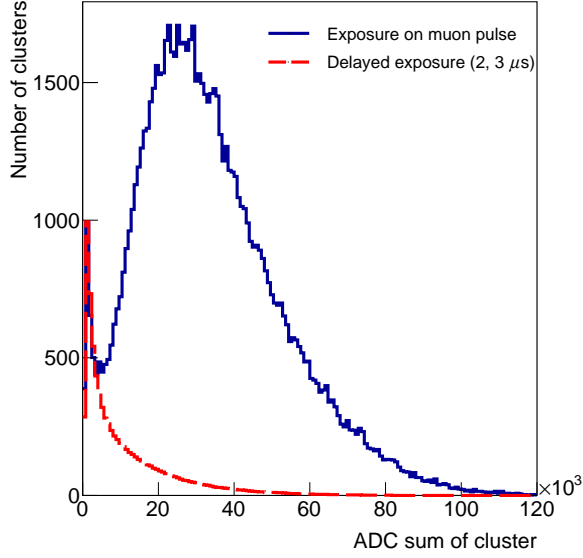Figure 4: Cluster ADC sum in 9×9 pixels for the exposure on muon pulse (solid) and the delayed exposure (dashed). Normalization is done for positron histogram by matching the first peak height with muon histogram
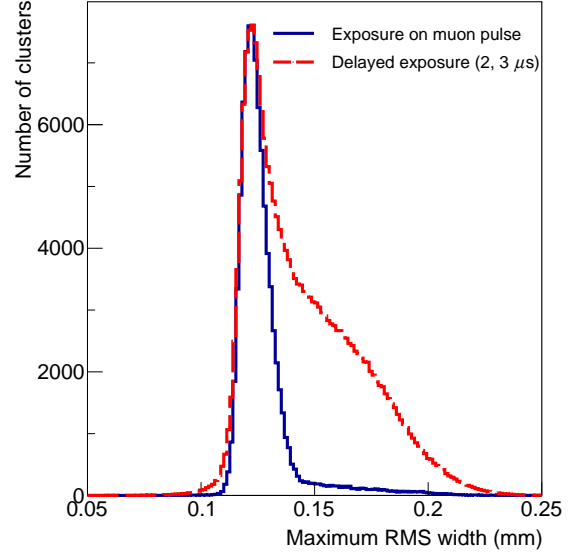

Figure 5: Signal's maximum RMS width histogram for the exposure on muon pulse (solid) and the delayed exposure (dashed) after rotating axes.

A positron signal pixel distribution can have a non-circular shape or even several peaks over the signal region because it can penetrate the MCP in any direction, since decay positrons are generated within the MCP with momenta in all directions. To parametrize the signal width, the minimum RMS width and the maximum RMS width of the clusters are calculated along the axes of each ellipse. The maximum width distribution is shown in Fig. 5.

For data in the muon beam time window, the maximum and minimum of the width distribution are almost the same, except for a small tail in the maximum width distribution. This is because the incident muon has mainly longitudinal momentum and makes a symmetric signal. For the delayed exposure data ($t_{delay} = 2, 3 \, \mu$s), the minimum width distribution is similar to that of the muon signal, but the maximum width distribution shows an excess at large RMS width value. Under the maximum RMS width cut ($\Gamma_{max} < 0.15 \, \text{mm}$), 57 % of the clusters in the delayed exposure survived while 94 % of the clusters in the muon pulse exposure survived.

The time distribution of the decay positrons should be described by an exponential decay function smeared by the time distribution of the incoming muon beam. In order to study the time distribution, data were taken by changing the trigger timing from $-0.5 \, \mu$s to $10 \, \mu$s with high intensity muon beam. The total ADC sum distribution versus the trigger time is shown in Fig. 6.

For a $500 \, \text{ns}$ exposure, 11 % of the stopped muons are expected to decay to the positrons within the exposure. The contribution of the decay positrons to the BPM signal is deduced from the total ADC sum distribution. The exponential function is fitted to the data in the time region later than $2 \, \mu$s, in order to avoid the contributions of incident muons. The measured decay parameter $\tau_\mu = 2.12 \pm 0.09 \, \mu$s agrees with the muon lifetime. The fraction of the positron contribution to the total ADC sum, ε, is $2.51 \pm 0.17 \, \%$.

The number of muons reaching the BPM has been estimated from the total ADC sum. The necessary calibration has been obtained from the analysis of low intensity muon beam data where the response of each individual particle (μ^+ or e^+) is identified. The average ADC count generated by a single cluster, a, is obtained by dividing the total ADC count by the number of detected clusters in the CCD image.

The parameter a from the data in the muon arrival time window is insufficient for the estimation of the number of muons because it contains contributions of both muons and decay positrons. On the other hand, the data taken after some delay
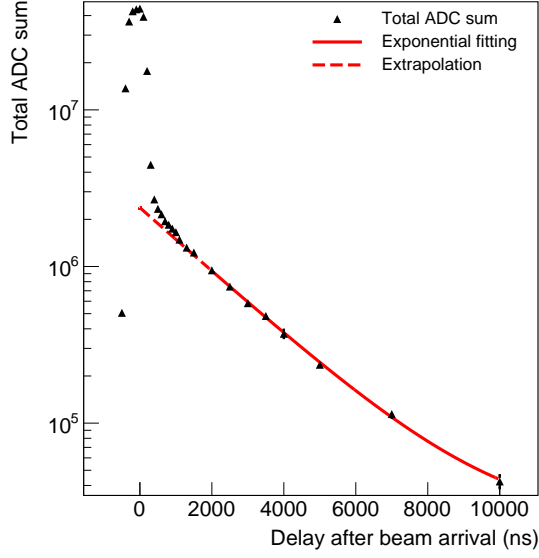
4

Figure 6: The time distribution of BPM signal intensity with different trigger time. An exponential function is fitted from 2000 ns to 10 000 ns and extrapolation to 0 ns is shown.
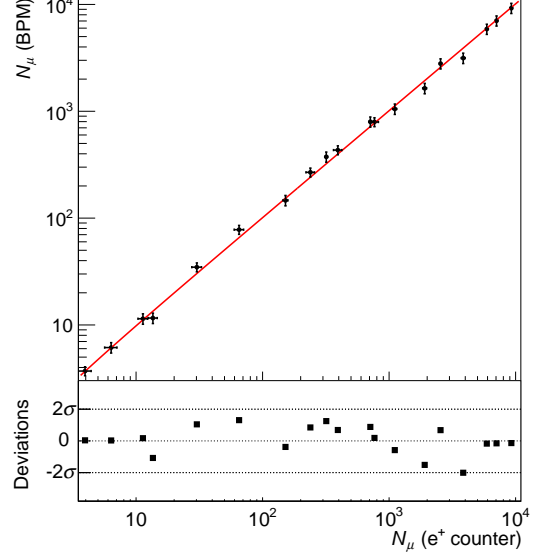

Figure 7: Estimated number of muons from BPM vs estimated number of muons from positron counter. Bottom graph shows residual distribution divided by error.

from muon arrival contain contributions primarily from decay positrons. By applying cluster analysis to this delayed data, the average ADC count generated by a single cluster of positron, a_e, is obtained. For estimating the number of positron clusters out of the total number of clusters, the a_e value is used together with ε, the measured ADC fraction of positron signal.

The total ADC sum in each picture, A, is measured from data at various muon beam intensities taken in the muon beam time window. The number of total clusters is calculated as A/a. In this way, it is possible to obtain the number of total clusters even when it is not possible to distinguish a single cluster due to the high muon beam intensity. On the other hand, εA is considered as the ADC contribution from the positrons. Thus, the number of clusters generated by the positrons is also estimated as $\varepsilon A/a_e$. Then, the rest of clusters are considered to be generated by muons. The number of muon clusters C_μ is calculated with this reasoning, $i.e$

$$C_\mu = C_{total} - C_e = A/a - A\varepsilon/a_e. \qquad (1)$$

It is reasonably assumed that one muon generates only one cluster since the transverse momentum of the muon is sufficiently limited by the upstream collimator. Therefore, the calculated number of muon

clusters is taken as the number of muons detected by the BPM, $N_\mu(\mathrm{BPM})$, shown in the vertical axis of Fig. 7.

An another independent estimation of the number of muons is made from the number of positrons detected by the positron counter located next to the BPM chamber. The proportionality constant has been obtained from the simulation based on the actual experimental setup implemented in the GEANT4 library [?]. The simulation estimates the number of muons on the MCP from the number of positrons detected by the positron counter in coincidence with muons.

The comparison of the number of muons obtained by these two independent methods at various beam intensity is displayed on Fig. 7. The detected muon beam intensity ranges from a few muon to 10^4 muon per bunch with three different sizes of collimator hole and several settings of slits in the beam line.

The statistical and systematic uncertainties are considered as follows. The major systematic uncertainties are from non-uniformity of gain ($\sim 4.4\,\%$), trigger timing uncertainty ($\sim 3.8\,\%$), positron background fitting ($\sim 5.6\,\%$) and inside light reflection ($\sim 2.4\,\%$). The statistical uncertainty is ten times smaller than systematic uncertainties except for the low intensity data where the statistical error is about $10\,\%$ for $N_\mu(e^+$ counter). The total error

is calculated as a quadratic sum of above uncertainties. It ranges from $9.6\,\%$ to $11.2\,\%$ for N_μ(BPM) and $1.7\,\%$ to $11.7\,\%$ for $N_\mu(e^+$ counter).

A first order polynomial function is fitted to data. Most measurements agreed well with fitting function within 2σ. The fitted slope is 1.01 ± 0.03. No evidence of saturation is observed.

4. Spatial resolution

The expected muon beam spot size during the first stages of muon re-acceleration is a few millimeters. Sharp-edge pictures were taken with a collimator and UV light source to estimate the BPM spatial resolution. Usage of the UV light allows one to avoid the positron background inevitably related to muons.

The half-circle open $0.5\,\mathrm{cm}$ thick stainless collimator was placed at $1\,\mathrm{cm}$ from the MCP front surface such that the collimator's edge was near the MCP center. The UV light provided by the Xe-lamp source was guided by optical fibre to the vacuum chamber. The light guide output was centered with the main MCP and collimator axis with distance along this axis about $15\,\mathrm{cm}$. Thus the collimator cast a sharp shadow on the MCP, and the image of the illuminated MCP surface produced a signal to be analyzed for estimation of the spatial resolution.

The collimator edge image was aligned to pixel rows by picture rotation and one pixel thick vertical slices were obtained (see Fig. 8). Discrete differentiation was applied to each slice. The peak, which corresponded to the location of the collimator edge, was emphasized by Hann function multiplication. The modulation transfer function was evaluated by fast Fourier transformation. The $10\,\%$ height frequency $\nu_{10\,\%}$ was obtained using a polynomial approximation to additionally suppress statistical fluctuations. More detailed information on the UV light resolution study is found in Ref. [?]. $\nu_{10\,\%}$ corresponds to a spatial resolution of $\Delta_\gamma = 0.29\,\mathrm{mm}$, which should be considered as an upper limit due to light reflection from the edge's surface induced by collimator and UV fiber misalignment.

The spatial resolution upper limit for muons is considered to be similar since the signal from single particles has almost the same width: $\Gamma_\mu/\Gamma_\gamma = 1.04 \pm 0.10$. Such a resolution satisfies the accelerator requirements.
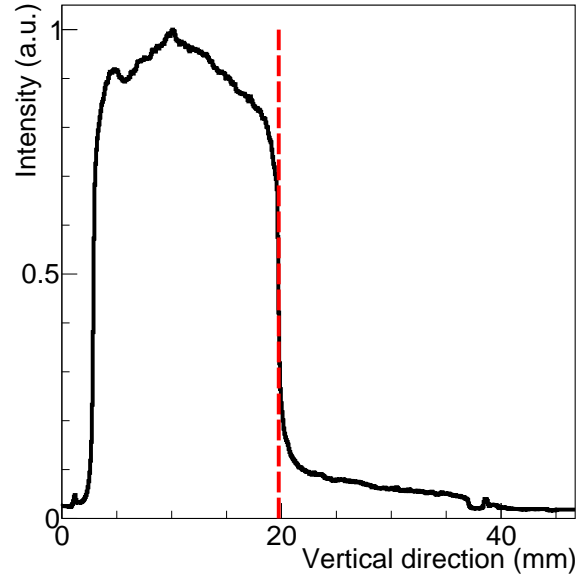

Figure 8: Projected ADC count distribution for UV light data on Y-axis following rotation to align the pixel orientation with the straight edge of the half circle collimator.

5. Conclusion

An MCP-based BPM has been developed to measure the profile of the ultracold muon beam for the J-PARC muon $g - 2$/EDM experiment. The BPM has been tested and evaluated by a surface muon beam and also by a UV light source. The spatial distribution of a muon beam was measured with this BPM with a high signal to background ratio between muon and positron signals. The positron background rate has been reduced to a negligible level using a short exposure window for the CCD camera and the additional selection of cluster characteristics on the CCD image. Good linearity was confirmed without noticeable saturation from a few muons to 10^4 muons. The spatial resolution was estimated as less than $0.30\,\mathrm{mm}$ from the UV light data.

References